https://doi.org/10.1590/jatm.v17.1384 ORIGINAL PAPER

Feasibility Assessment of Unmanned Aerial Systems for Precision Approach Path Indicator Inspections: a Cost-Effective and Sustainable Alternative

Alex Sandro Mendes Tostes[1], Leonardo Marini-Pereira[1*], Alison de Oliveira Moraes[2], Leandro de Oliveira Peixoto[1], Gabriel Dietzsch[3], Cristian da Silveira Smidt[1], Marielcio Gonçalves Lacerda[3], Mateus Habermann[4]

1. Departamento de Controle do Espaço Aéreo – Instituto de Controle do Espaço Aéreo – Divisão de Pesquisa – São José dos Campos/SP – Brazil.
2. Departamento de Ciências e Tecnologias Espaciais – Instituto de Aeronáutica e Espaço – Divisão de Eletrônica – São José dos Campos/SP – Brazil.
3. Departamento de Ciências e Tecnologias Espaciais – Instituto de Estudos Avançados – Divisão de Comando e Controle, Computação, Comunicação, Inteligência, Vigilância e Reconhecimento – São José dos Campos/SP – Brazil.
4. Departamento de Ciências e Tecnologias Espaciais – Instituto Tecnológico de Aeronáutica – Programa de Pós-Graduação em Aplicações Operacionais – São José dos Campos/SP – Brazil.

*Correspondence author: marinilmp@fab.mil.br

ABSTRACT

The use of unmanned aerial platforms has increasingly been demanded in various applications. Among these, in-flight inspection stands out, traditionally conducted by aircraft equipped with various sensors to verify the performance requirements of ground-installed navigation aids, as well as air navigation procedures for operational and airworthiness purposes. In-flight inspection is costly in terms of time, qualified personnel, necessary equipment, flight hours, and operational impact on the inspected aerodrome. In this context, the use of unmanned aerial systems (UAS) emerges as a potentially cost-effective alternative, with the potential to significantly reduce the costs associated with the in-flight inspection of navigation aids. This work presents the methodology and results of in-flight inspection of the precision approach path indicator (PAPI) using UAS. The results presented are selected from over a dozen field campaigns, wherein inspection procedures were adapted to replace conventional aircraft with UAS. The results were compared to traditional inspections performed by the conventional aircraft crewed with professional flight inspectors. The findings indicate a strong similarity between the UAS methodology and conventional inspection, suggesting that UAS could partially or completely replace conventional inspections, significantly reducing the time, costs, and impact of inspections carried out by conventional aircraft.

Keywords: Unmanned aerial vehicles; Flight inspection; Precision approach path indicators; Navigation aids; Automation; Statistical analysis.

INTRODUCTION

The inspection of navigation aids is a critical component of flight inspection, ensuring the accuracy and reliability of systems essential to aviation safety and operational efficiency, as well as compliance with international standards for aviation safety. Conventional navigation aids, specifically the instrument landing system (ILS), distance measuring equipment (DME), and

Received: Feb. 12, 2025 | **Accepted:** Apr. 02, 2025
Peer Review History: Single Blind Peer Review.
Section editor: Paulo Renato Silva

precision approach path indicator (PAPI), provide critical guidance to pilots during specific phases of flight, such as approach and landing. These systems must be properly functioning to uphold safety with respect to the stringent International Civil Aviation Organization (ICAO) standards. Conventional verification typically uses specialized equipment onboard an aircraft, carried out by a pilot trained for flight inspection alongside a dedicated crew that verifies measurements from ground-based navigation aids. However, conventional methods for in-flight inspection present a significant operational challenge: dependence on crewed aircraft equipped with specialized sensors. These operations incur substantial ongoing costs such as aircraft maintenance, fuel consumption, and investments in specialized training for personnel. Furthermore, extended flight durations paired with high fuel demands result in considerable carbon emissions, contributing to environmental concerns and requiring solutions compatible with sustainability goals.

For example, an Embraer Legacy 500 aircraft, typically used for flight inspection, consumes approximately 287 gallons (1,086 liters) of fuel per hour (Guardian Jet 2022). Over a 30-minute inspection flight, it burns around 143.5 gallons (543 liters) of fuel, resulting in approximately 1,713 kilograms of CO_2 emissions, considering the standard emission factor of 3.15 kg CO_2 per kilogram of fuel burned (Brasil 2010). The provided example determines conventional flight inspection contribution to the environment and points out the need for greener alternatives.

Another serious limitation with conventional flight inspection is the operational disruption they cause at airports. In many instances, normal airport activities have to be stopped or curtailed to make way for the inspection flights, which results in a number of logistical complications and possible financial losses. This dependence on manned aircraft also creates safety hazards, especially when the operations are around busy or complicated airspace due to operational complexities involved (Borges *et al.* 2024). For example, when a flight inspection is conducted to validate a glide slope, it may need specific aircraft configurations or maneuvers that require temporary airspace restrictions. This can disrupt normal traffic patterns, leading to increased risk of airspace conflicts or delays, especially if not carefully coordinated with air traffic control. Additionally, the inspection aircraft, flying non-standard patterns, may heighten the workload and complexity for air traffic controllers, potentially impacting overall traffic flow and safety. The challenges mentioned create an urgent need for the development of more cost-efficient, eco-friendly, and operationally effective solutions to complement or even replace traditional flight inspection methods.

Additionally, air navigation has undergone a major overhaul recently, with the advanced technologies of navigation coming into widespread application, such as performance-based navigation (PBN). The driving force behind these changes has been the integration of global navigation satellite systems (GNSS), which enhances the precision, efficiency, and flexibility of flight operations. The modern navigation enables aircraft to follow more direct routes – saving fuel, hence minimizing their operational cost and impact on the environment. However, the adoption of these technologies necessitates a rigorous focus on safety measures, especially in critical procedures such as required navigation performance (RNP) approaches, where ensuring operational reliability and mitigating risks are paramount (Oliveira *et al.* 2023; Rodrigues *et al.* 2022).

Among others, systems such as ground-based augmentation systems (GBAS) have revolutionized approach and landing procedures by providing highly accurate positioning data, enabling precision approaches even in challenging environments, as discussed by Marini-Pereira *et al.* (2021), Monico *et al.* (2022), and Sousasantos *et al.* (2021). The introduction of GNSS-based solutions has set a new standard for air navigation, significantly improving efficiency and operational capabilities. Similarly, unmanned aerial systems (UAS) hold the potential to bring a comparable transformation to flight inspection operations by offering flexible, cost-effective, and scalable solutions. As the reliance on GNSS-based navigation increases, the demand for rigorous and frequent validation of navigation aids continues to grow, emphasizing the need for more efficient and adaptive inspection methodologies. Investigating innovative solutions such as UAS becomes vital to addressing the evolving requirements of modern air navigation while ensuring compliance with stringent performance standards.

Unmanned aerial systems (UAS) are increasingly utilized across a multitude of civil applications, including remote sensing, surveillance, precision agriculture, and disaster management, due to their cost-effectiveness, operational flexibility, and ability to access challenging environments (Sivakumar and Tyj 2021). UAS offer a host of advantages over traditional methods: reduced operation costs, no adverse environmental impacts, and flexibility in deployment. Unlike the conventional crewed aircraft, the UAS is allowed to fly within restricted airspaces and under conditions that might otherwise be prohibitive for manned operations.

Unmanned aerial systems (UAS) fitted with high-resolution cameras and advanced GNSS/real-time kinematic (RTK) positioning technologies offer great data with high accuracy; thus, they enable real-time monitoring and analysis. These capabilities make UAS cost-effective, scalable solutions to meet the ever-increasing demand for reliability and efficiency in flight inspections. Despite such advantages, several challenges must be overcome to achieve full-scale adoption of the transition toward UAS-based inspections. Regulatory compliance is a major concern: most of the existing frameworks are targeted at conventional aircraft and may not fully accommodate UAS operations. In other words, the established regulatory structures and guidelines were designed for conventional manned aircraft operations. These frameworks typically include airworthiness certification, flight operations, airspace management, pilot licensing, among other aspects.

This, of course, requires the collaboration of aviation authorities to ensure compliance with ICAO standards and the establishment of appropriate policies that will ensure safety and reliability. Additionally, challenges related to the accuracy of positioning systems, data processing techniques, and the validation of the results of the inspection performed using UAS inspection compared to traditional methods need to be carefully assessed. This process requires the development of robust methodologies and validation frameworks that ensure consistency and reliability of data across different operational scenarios, for the same level of precision as manned inspections. This research aims to evaluate the feasibility of using UAS for PAPI inspections by adapting traditional inspection methodologies to UAS platforms and assessing their accuracy and reliability. It considers whether the UAS-based inspections can provide results comparable to traditional methods and thus allow for partial or total migration to unmanned operations. The paper shows in detail the data acquired from test campaigns carried out for performance indicators such as precision, repeatability, and efficiency of operations evaluation.

At the time of the field campaigns, this work represents the pioneering initiative in Brazil to conduct a field trial and propose a methodology for using UAS to aid in the flight inspection of PAPI systems. It represents the proof of concept and shows the technical feasibility of using UAS for flight inspections, presenting some advantages. The methodology employed in this research distinguishes itself by requiring only standard equipment: a UAS equipped with RTK, a camera compatible with the activity, and data processing software, eliminating the need for additional specialized hardware. The findings present insight into practical applications and limitations experienced with UAS technology in this area. The successful integration of the UAS into routine inspection procedures could result in substantial cost savings, increased operational efficiency, and enhanced safety relating to aviation infrastructure management.

PRECISION APPROACH PATH INDICATOR (PAPI)

The PAPI is a well-established yet critical visual aid system at airports, providing approach guidance that precedes the landing phase of flight. It consists of a set of lights aligned alongside the runway, visually indicating the aircraft's vertical position relative to the optimum approach path, which is typically set at a 3° glide slope. As highlighted by Yadav *et al.* (2022), the approach and landing phases account for a significant proportion of flight-related incidents, underscoring the importance of reliable guidance systems such as PAPI. This system complements the glide slope component of the ILS, which provides radio frequency (RF) guidance. In other words, while the ILS glide slope offers an approach path through RF transmission, the PAPI provides visual guidance via a specific arrangement of lights positioned laterally along the runway, ensuring a safe and stable descent.

The PAPI system consists of four light boxes containing a light source, filters, and lenses that provide an observer on the optical axis above a white color indication of light while a below-optical-axis observer perceives a red indication. Figure 1 highlights some components in the PAPI light box to realize the indication provided in such visual perception.

With the features of the light box as shown in Fig. 1, a series of four boxes are set at different angles, which are slightly above and below the nominal 3° approach path. In such an arrangement, a pilot in the approach phase can tell whether their rate of descent is more or less than what is required for landing safely. It also means that through a combination, precision approach path indicator (PAPI) lights provide critical feedback on whether the aircraft is on or off the glide slope and when it needs adjustment to maintain an ideal trajectory in descent.

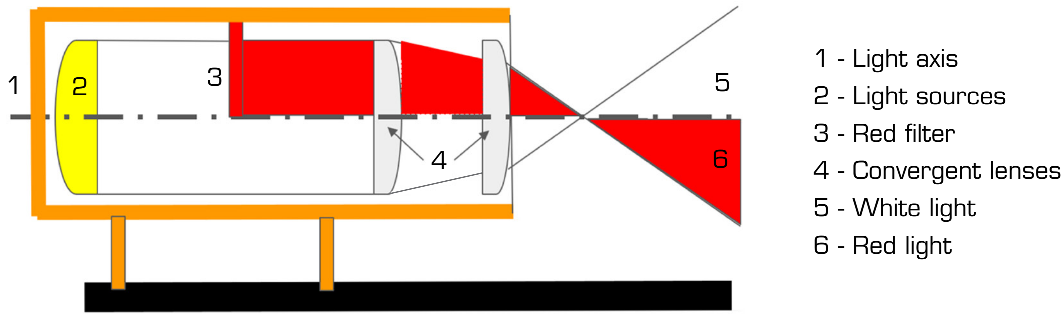

Source: Adapted from Wikipedia (2023).

Figure 1. Components of a PAPI light box.

By placing the light boxes at different inclinations, the system generates a narrow conical beam. Two white lights and two red lights viewed together indicate that the aircraft is on the correct 3° approach path. Figure 2 shows the PAPI lights arrangement and the angles' relation to providing a standard 3° glide path.

The PAPI system provides the pilot with distinct visual clues in a very intuitive manner. If the pilot sees two white lights and two red lights, this means the aircraft is on the right glide path. If more white lights than red lights are visible, this implies that the aircraft is above the ideal glide path and should correct its course by descending. Conversely, if there are more red lights than white ones, this means the aircraft is below the optimal glide path and should therefore climb. Figure 3 depicts the mentioned combinations of lights along with the aircraft condition: up, below, or in the glide path.

It is important to emphasize that in a standard four-light PAPI system, each light box is calibrated individually, with each box providing a different angle, typically slightly above or below the nominal 3° approach path. The specific angles for each box in the nominal case are detailed in Fig. 2. This calibration provides precision and compliance with regulatory approaches, thereby contributing to flight safety during the landing phase.

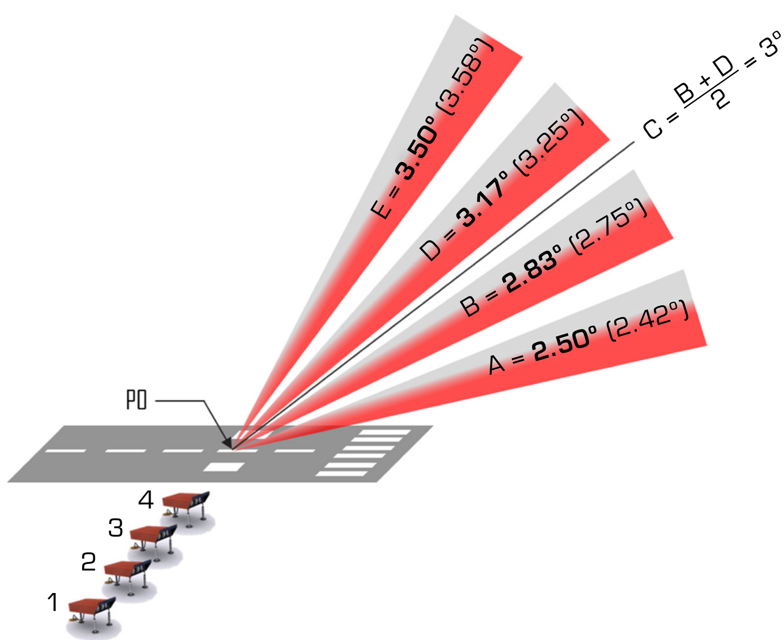

Source: Adapted from Brasil (2023).

Figure 2. Precision approach path indicator (PAPI) light arrangement for a 3° approach path. The identified angles from the PO are the following: A: low transition; B: medium-low transition; C: nominal ramp; D: medium-high transition angle; and E: high transition. Angles in parentheses are standard values for ILS-connected installation and for large aircraft.

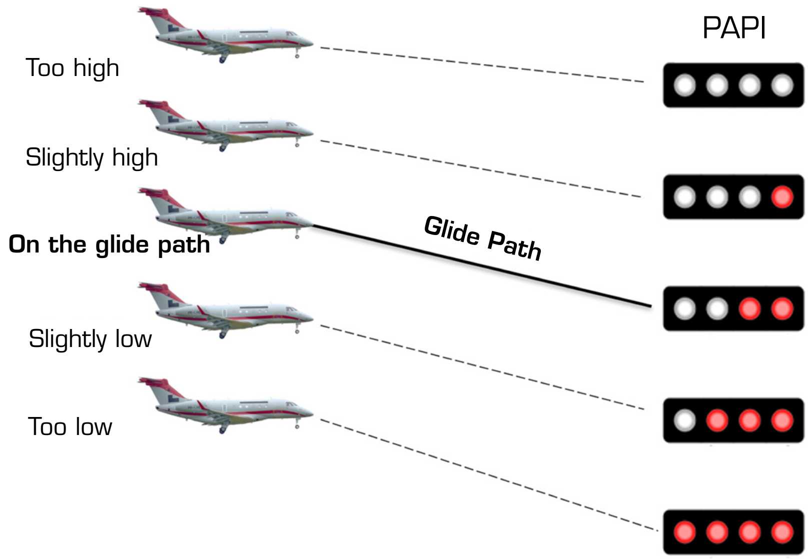

Source: Elaborated by the authors.

Figure 3. Precision approach path indicator (PAPI) light configuration indicating correct descent rate.

Conventional PAPI inspection

The traditional method for in-flight inspections of PAPI relies on the use of a theodolite to measure the angles of the PAPI light boxes. The execution of this requires close coordination between the aircraft crew and the ground inspection team operating the theodolite (Brasil 2023). The ground team positions the theodolite on a geodetically known position on the side of the runway, near the PAPI light boxes. The operator points the theodolite to the aircraft's nose (radome), while another team member, located nearby, contacts the flight crew on very high frequency (VHF) radio. Figure 4 depicts the process out of scale, meaning that the relative distance between the aircraft and the operators is much larger than shown in the figure.

The ground team is provided with the desired transition angles for each PAPI light box and the nominal glide slope angle. When the flight crew observes a light transition – that is, from red to white or vice versa – they call the event to the ground team

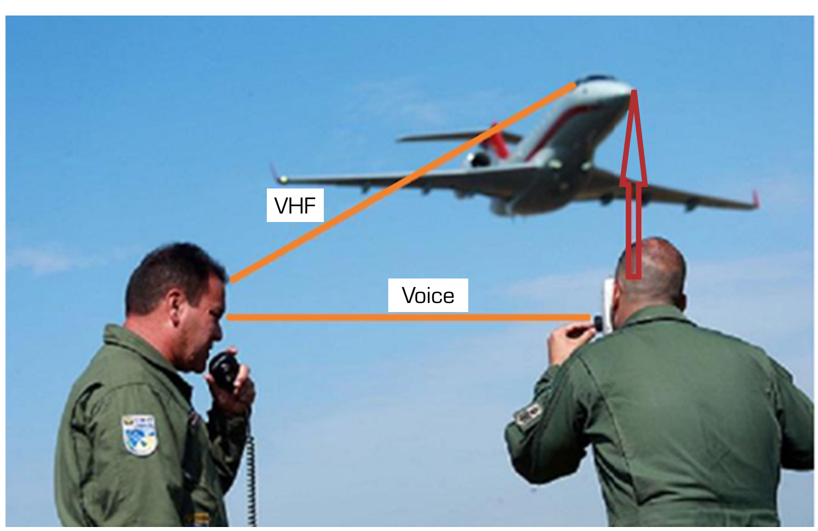

Source: Elaborated by the authors.

Figure 4. Theodolite-based PAPI inspection method, where the ground operator aligns the theodolite with the aircraft's nose (radome), while a team member communicates with the flight crew via VHF radio for coordination.

over the radio. The ground operator records the angle corresponding to the event and reads the data back to the flight crew for verification. In summary, the main goal of the inspection flight is to determine the inclination angle of each PAPI box, with the nominal 3° approach path values provided in Fig. 2.

The flight inspection team applies specific flight profiles to perform the vertical and horizontal scanning relative to the installation of the PAPI light box. These are called Pattern 2, Pattern 3, and Pattern 4.

The Pattern 2 profile includes runs where the aircraft maintains a constant altitude while flying toward and away from the PAPI system from predefined points. In some cases, the flight path deviates laterally from the runway's extended centerline. This operational profile is illustrated in Fig. 5.

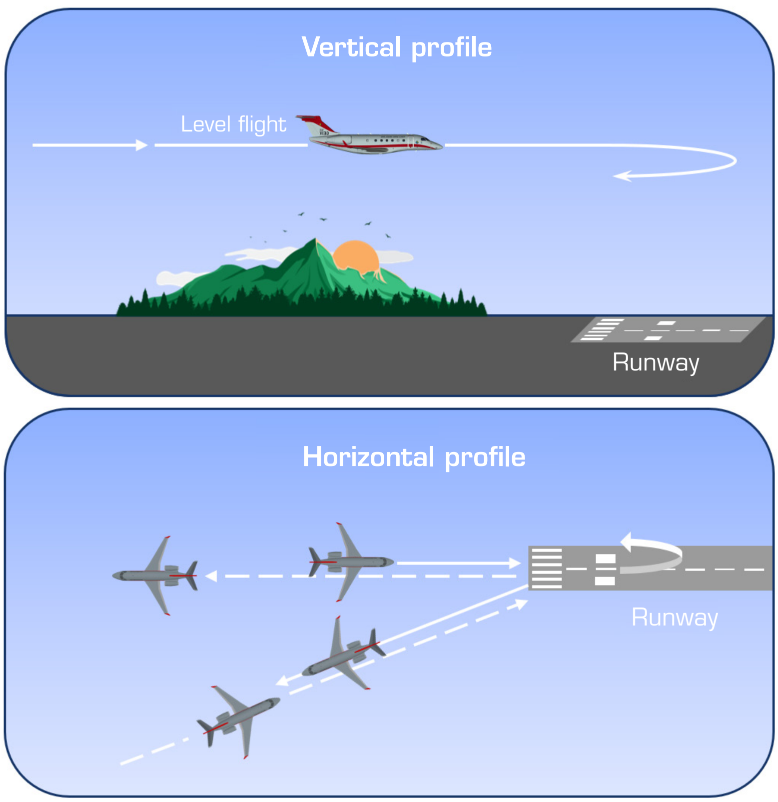

Source: Adapted from Brasil (2023).

Figure 5. Flight profile Pattern 2 for vertical inspection.

The Pattern 3 profile type encompasses approach flights directed towards the runway, which follow a go-around maneuver slightly beyond the outer marker (OM) or over the threshold, typically deviating laterally from the extended runway centerline. This profile type is illustrated in Fig. 6.

Pattern 4 runs are performed parallel to the runway approach axis, crossing the OM at a specified altitude. This pattern facilitates an angular inspection extending up to 45 degrees on either side of the extended runway axis. Figure 7 depicts this profile, where 2 NM indicates a two-nautical-mile distance.

Each of these flight profiles enables comprehensive testing of the PAPI system, including verification of transition angles, glide slope width, and horizontal coverage. Though highly effective, the conventional method involves substantial operational costs, extended flight hours, and significant fuel consumption. These factors highlight the importance of exploring complementary solutions, such as UAS, which could potentially reduce the frequency of these resource-intensive procedures while maintaining inspection reliability.

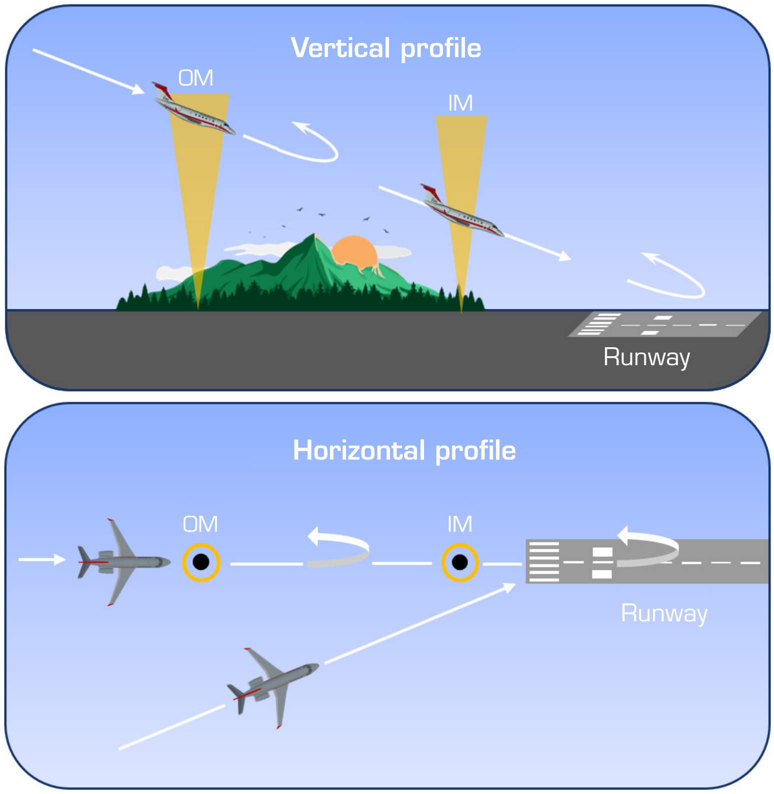

Source: Adapted from Brasil (2023).

Figure 6. Pattern 3 run profile with go-around maneuvers. IM = inner marker.

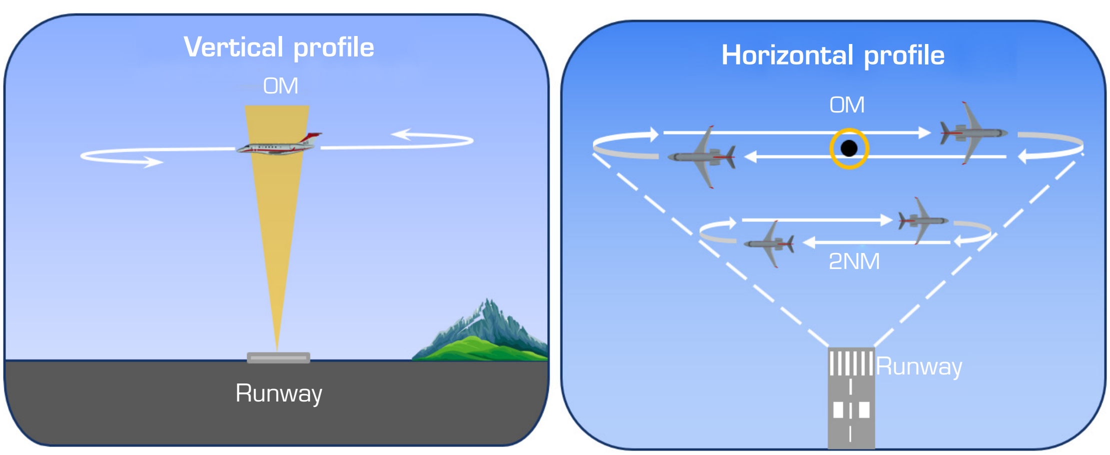

Source: Adapted from Brasil (2023).

Figure 7. Flight profile for Pattern 4, horizontal sweep.

FLIGHT INSPECTION OF NAVIGATION AIDS USING UNMANNED AERIAL SYSTEMS (UAS)

Recently, a boost in the use of UAS has been observed across various applications, including their possible use for the flight inspection of navigation aids. Increasing demands for a cost-efficient, effective, and environmentally friendly substitute for the traditional methods of flight inspection have been driving research efforts to investigate the feasibility of UAS-based inspections. Several studies have been conducted to evaluate different methodologies focusing on the inspection of the PAPI system.

Unmanned aerial systems (UAS)-based flight inspection approaches

Rahnama *et al.* (2018) introduced the pre-flight inspection methodology for ILS and PAPI using UAS to reduce the flight hours of manned aircraft and increase the frequency of inspections. Correspondingly, their approach employs a precision clinometer or theodolite equipped with a laser in combination with an RTK-enabled UAS. This laser beam, calibrated for accuracy in accordance with ICAO DOC 8071, provides the necessary precision for this application. For ILS inspections, a laser-aligned sensor (accurate within 20 arc-seconds) is integrated with an NM 7710 onboard ILS analyzer. This system transmits real-time data via a wireless link back to the ground processing team for final processing and systems adjustments. The PAPI inspections are supported by placing a laser emitter parallel to the PAPI alignment where the beam would be adjusted against each light box in turn. The UAS intercepts the laser signal, recording its position and capturing images of the lights.

Lin *et al.* (2020) developed a UAS-based inspection system using a prism mounted adjacent to the UAS camera and two types of total stations to independently measure angles and distances. Tests were conducted at Purdue University Airport using both manual (Topcon ES-105) and automated (Trimble S7) stations, along with a GNSS-RTK receiver (Trimble R10) for establishing ground control points. Georeferencing of the acquired images was performed with a prism and total stations while transition angles were derived using triangulation and multinomial logistic regression. Results indicated that for light boxes 1 and 2, the measurements were within the tolerance limit, but changes in boxes 3 and 4 were needed.

Sommer *et al.* (2020) investigated the application of a low-cost UAS fitted with a software-defined radio (SDR) platform for the inspection of ILS and VHF omnidirectional range (VOR) systems. Their system employed a Jetson TX2 embedded computer to process the incoming signals and transmit data to a ground station. The regulatory constraints entailed testing the concept in two stages: autonomous flights of UAS on a predefined trajectory and tests conducted while having the UAS system fixed on a vehicle. The measurements show that an SDR system can effectively estimate modulation depth for both ILS and VOR signals, therefore proving the possibility of using UAS as support in inspection activities.

In contrast to previous studies, this manuscript presents the first demonstration of the feasibility of using UAS for PAPI system inspection in Brazil. Moreover, the approach used in this study sets itself apart by necessitating only standard equipment: a UAS with RTK, a camera suitable for the task, and data processing software, thus removing the need for extra-specialized hardware.

While research by Oliveira Costa *et al.* (2020) demonstrated the feasibility of using remotely piloted aircraft systems (RPAS) for VOR flight inspections by the Brazilian Air Force (Força Aérea Brasileira [FAB]), the application to PAPI systems specifically represents a significant innovation within the Brazilian context. This study validates the application of UAS for PAPI inspections, meeting regulatory requirements and demonstrating system compliance with standard regulations for PAPI flight inspection method calibration. The implementation of UAS for PAPI inspection in Brazil has the potential to reduce operational costs and increase inspection frequency without compromising the precision and reliability necessary for safe air navigation.

Economic, environmental, and safety considerations

The authors in Togola *et al.* (2021) investigated two inspection architectures, both using UAS for real-time and post-processing procedures, while considering economic, environmental, and safety aspects compared to traditional inspections. They estimated that UAS flying hours can be three times more cost-effective than crewed inspections and that acquisition costs were 10 to 15 times lower. Furthermore, carbon emissions could be reduced by up to fortyfold depending on the type of navigation aid and aircraft used.

Wilkens *et al.* (2018) initiated the development of a comprehensive UAS-based inspection system to evaluate various navigation aids such as ILS, VOR, and PAPI. These systems have a modular design with an onboard autopilot, RTK positioning, and RF signal receivers that can transmit in real time to a ground station. A commercial DJI Matrice 300 RTK was used because of its reliability and the possibility of software development inside. It also concluded that the application of identical software and databases for manned and UAS inspections facilitates transition and operational efficiency.

Advancements in image-based PAPI inspections

The test of Černý *et al.* (2022) approached the survey of abbreviated PAPI (APAPI) systems and runway lighting at a small uncontrolled airport for assessment purposes using commercial UAS. A very light DJI Mini 2 was tested along with a bigger one, the DJI Matrice 600 Pro, both carrying a high-resolution camera. With the purpose of providing data to the required flying altitude for conducting transition light measurements, the Mini 2 uses GNSS data while the Matrice 600 Pro relies on onboard barometers. It was concluded that thermal cameras can bring out light transitions better than RGB cameras and hence, they would improve measurement accuracy.

Rahnama and Asaadi (2023) compared UAS-based inspections with traditional crewed inspections, using an ILS/PAPI spectrum analyzer, model PIR361, integrated with RTK-based positioning for reference. Their results showed that the short-range operation of UAS can provide comparable accuracy with conventional methods and again pointed out the importance of a precise reference for minimizing errors.

Key findings and future directions

From the review of related literature, it would appear that UAS-based PAPI inspections are mainly based on imaging sensors, considering the visual nature of the aid. RTK positioning systems are often used to provide accurate positioning of the platform, thus enabling an effective calculation of transition angles of light. As highlighted by Nowak *et al.* (2022), the integration of vision-based systems with UAS platforms enhances the precision of approach and landing phases, further reinforcing their potential in inspection applications. The complementary use of UAS offers some advantages over traditional techniques, such as cost-effectiveness, including reduced operation and maintenance costs when compared to inspections by crews; environmental sustainability due to lower fuel consumption and emissions; operational flexibility, minimizing disruption to airport operations while enabling higher scheduling flexibility; and improved accuracy, achieved through advanced sensor integration and higher automation potential.

Despite these advantages, complete regulatory compliance, ensuring the accuracy of data, and integrating UAS operations within current flight inspection protocols still pose challenges. Further research is required in refining methodologies to enhance the precision of measurement, exploring the use of artificial intelligence (AI) for data analysis, and developing regulatory frameworks that allow for wide-scale implementation of UAS-based inspections.

METHODOLOGY FOR UNMANNED AERIAL SYSTEMS - BASED PAPI FLIGHT INSPECTION

This section presents the materials and methods used in this research, detailing one comprehensive methodology developed to establish the feasibility of executing PAPI flight inspections using UAS, by integrating expertise from a multidisciplinary team and utilizing specialized instrumentation.

Simulation and constraints

Before the experimental trials, a software-in-the-loop simulator was developed to analyze possible flight profiles. The operation of the UAS was planned to be conducted about 300 meters in front of the PAPI system and over the runway threshold. The simulator generated estimates of transition heights and lateral displacements required for the inspection process. Figure 8 shows the simulator interface. The left window gives a top-down view and pilot control panel; the right window provides a 3D view of the inspection scenario.

Complementary to the simulation, the recommendations of Section II, Item 13.8 of Chapter 13 (Checklist) from the Brazilian Flight Inspection Manual (Brasil 2023) were followed. The checklist defines the main items that should be checked during PAPI inspections:

- Transition angles and standard approach slope;
- Beam width;
- Light functionality, intensity, and visibility;
- Usable angular coverage;
- Contrast and clarity of the light beam;
- Obstacle clearance;
- Alignment with electronic precision glide slope; and
- Secondary power sources.

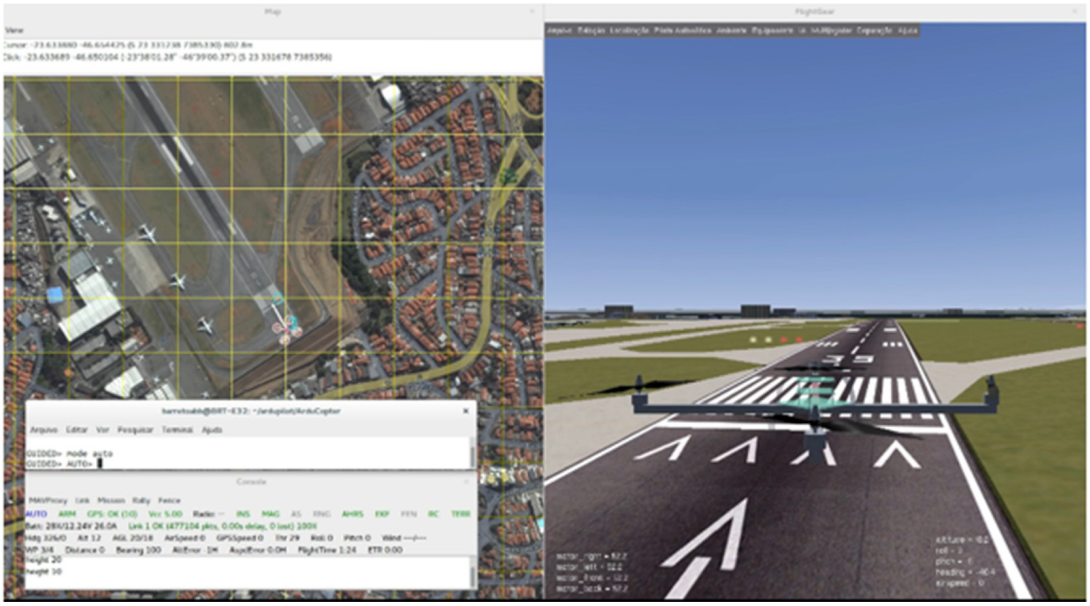

Source: Elaborated by the authors.

Figure 8. Unmanned aerial systems (UAS)-based PAPI inspection simulator interface.

However, certain aspects that cannot be verified through the proposed UAS-based methodology – such as obstacle clearance due to airspace restriction issues, electronic glideslope alignment due to equipment constraints, and secondary power sources – may require separate confirmation.

To address the feasible aspects, two sweeping techniques were employed using UAS:

- Vertical scanning – to assess the approach descent angle.
- Horizontal scanning– to evaluate the light beam's angular coverage.

The results obtained through the UAS inspections were compared to conventional manned inspections conducted by GEIV to validate accuracy and reliability. GEIV is the Portuguese acronym for the Brazilian flight inspection squad, named Special Group for Flight Inspection.

Descent angle analysis: vertical scanning

The vertical scanning method involves conducting flights upwards and downwards to capture all the PAPI light transitions, as shown in Fig. 9. From the coordinates of the point of origin (PO) and coordinates of the UAS, given by the RTK system, exactly in the transition position, the inclination for each PAPI box is estimated. To improve the detection of the transition by the optic system, a blue optical filter was used on the camera to enhance the visibility.

The vertical scanning procedure comprises the following steps:

- Make at least seven flight runs in each of ascent or descent.
- A ground operator observes real-time video and records points of transition.
- Position data from the UAS are automatically recorded at every instant of transition.
- A final report is produced giving calculated approach angles.

It was found that at least five measurement runs per session are required, with better results from a larger measurement set. However, data from as few as three measurements, and at least three runs may achieve results comparable to traditional inspections.

Angular coverage analysis: horizontal scanning

To evaluate the horizontal coverage of the PAPI, two distinct methodologies can be employed. The joint scanning (Figs. 10 and 11) involves moving the UAS parallel to the alignment of the PAPI boxes. During this process, two key events are recorded:

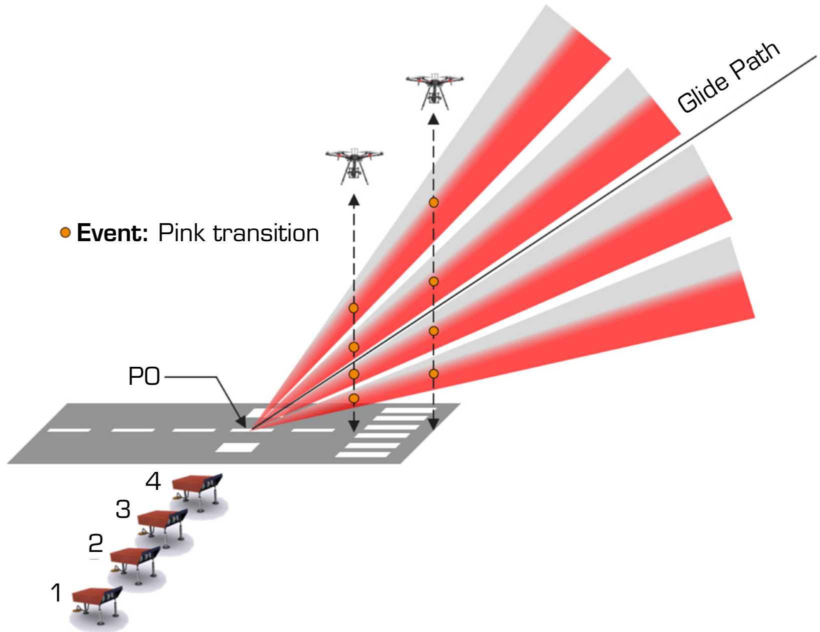

Source: Elaborated by the authors

Figure 9. Vertical scanning method for descent angle verification.

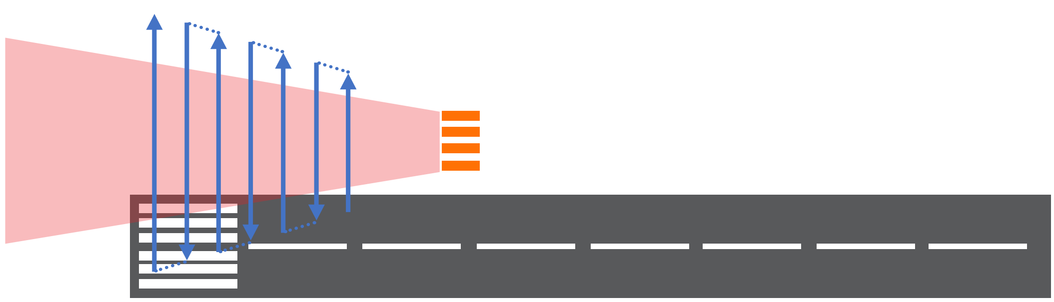

Source: Elaborated by the authors.

Figure 10. Illustration of incremental horizontal scanning showing the UAS moving laterally to the initial position.

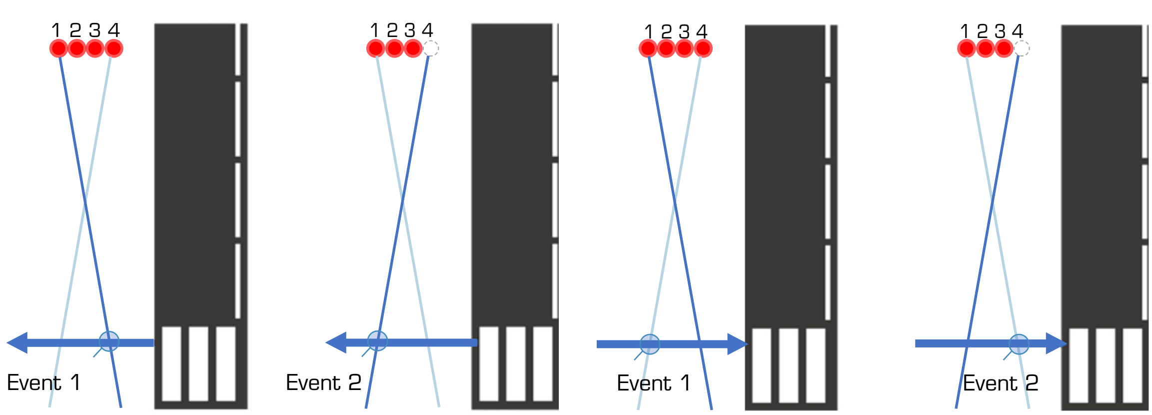

Source: Elaborated by the authors.

Figure 11. Events of incremental horizontal scanning: instant when all lights are turned on (Event 1) and first light is switched off (Event 2).

Event 1, when all lights in boxes 1 through 4 are illuminated, and Event 2, when the light in box 1 turns off. The UAS is then flown until all lights are extinguished, resetting the system for the next measurement.

To ensure the accuracy of the data collected, the UAS is progressively flown further away from the system, as illustrated in Fig. 10. It is recommended that this procedure be repeated at least seven times to minimize measurement errors and establish a reliable average.

The objective is to determine the angular coverage of the PAPI, indicated in magenta in Fig. 10. Notably, this coverage should be assessed when all lights are visible, meaning that consideration must be given to the point at which the opposite box's light first becomes visible.

In turn, the individual box scanning involves moving the UAS parallel to the alignment of the PAPI boxes, with an initial focus on box 4, observing its lamp turning on and off (Figs. 12 and 13). After collecting data from box 4, the process was repeated for box 1. This method is useful when dealing with differing lighting conditions, or when consistent data is not obtainable using the joint scanning method.

This process places the UAS at the location where all the lights are off. The UAS is then moved laterally until the light on the targeted box, either 1 or 4, turns on. Then the UAS moves further away from the PAPI and is displaced in the opposite direction until the light goes off. The process is repeated a number of times for the purpose of ensuring precision of measurement.

Like the previous method, multiple runs are required to increase the accuracy of the measurements. Nevertheless, three runs can be enough to achieve consistent results.

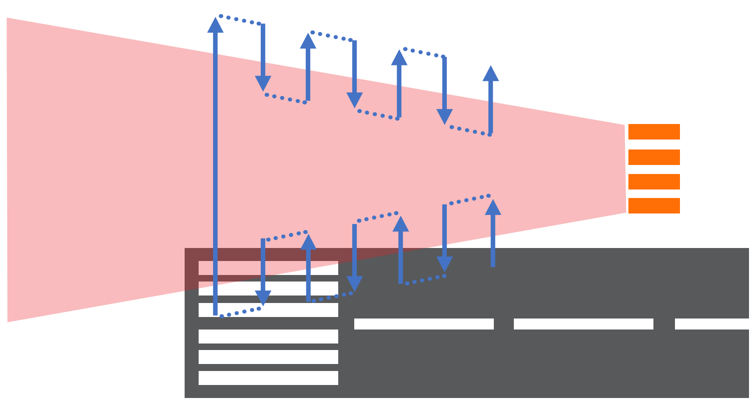

Source: Elaborated by the authors.

Figure 12. Lateral-horizontal incremental scanning illustration with individual analysis of light boxes 1 and 4.

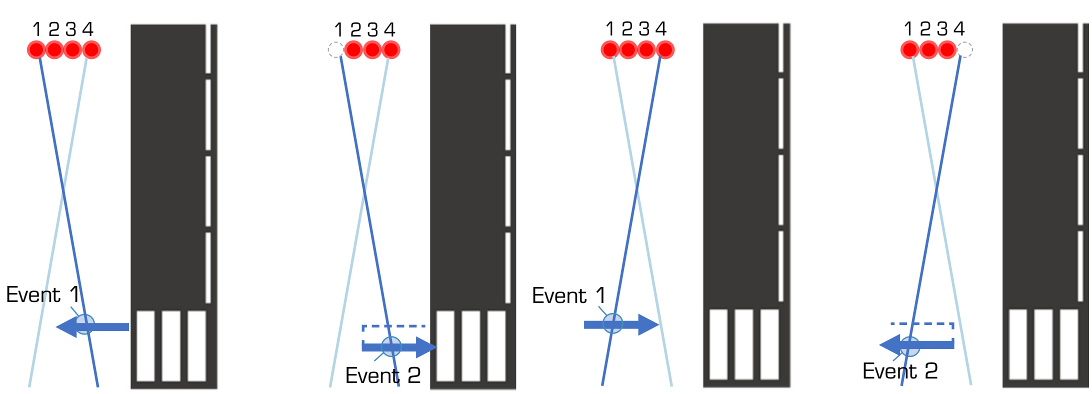

Source: Elaborated by the authors.

Figure 13. Events of incremental horizontal scanning: instant when all lights are turned on (Event 1) and first light is switched off (Event 2).

EQUIPMENT USED

Data collection was performed using the DJI Matrice 600 PRO (DJI 2020), shown in Fig. 14, which is equipped with RTK positioning, assuring high-precision 3D location accuracy. The camera mounted on the drone was a Nikon D3100, using the original gimbal system to capture images in high resolution. Table 1 specifies in detail the technical specifications of the UAS used in this research work.

Source: Elaborated by the authors.

Figure 14. DJI Matrice 600 PRO used during this study.

Table 1. Technical specifications of DJI Matrice 600 PRO.

Feature	Description
Payload capacity	Can carry heavy loads up to 6 kg, making it suitable for professional cameras and other equipment.
Flight time	Equipped with six batteries, providing up to 32 minutes of flight time without payload and up to 16 minutes with maximum payload.
A3 Pro Flight controller	Enhanced with triple modular redundancy and diagnostic algorithms for greater reliability and precision.
HD Lightbridge 2 Transmission	Supports long-range high-definition video transmission (up to 5 km), ensuring clear and reliable communication.
Power management	Integrated battery management system that monitors real-time status and ensures a stable power supply.
Gimbal compatibility	Compatible with Zenmuse gimbals (such as Z15, X3, X5, X5R, and XT) and supports the Ronin-MX gimbal for professional camera setups.
Smart flight modes	Supports multiple intelligent flight modes, including waypoint navigation, point of interest, and active tracking for automated flight planning and execution.
Redundant design	Redundant systems, including inertial sensor units and GNSS modules, ensure higher safety and reliability.
SDK compatibility	Compatible with DJI Software Development Kit (SDK) for developing custom applications, allowing tailored solutions for industrial needs.
Imaging	Supports a wide range of cameras and sensors, including high-resolution cameras for mapping, inspection, and surveillance applications.
GNSS+RTK	Dual GPS and GLONASS positioning systems with RTK support for precise positioning and navigation.
Comprehensive safety features	Includes safety mechanisms such as return-to-home, low battery warning, and obstacle avoidance.

Source: DJI (2020). GLONASS = Globalnaya Navigazionnaya Sputnikovaya Sistema; GPS = Global Positioning System.

An optical filter was tried for better light transition detection; thus, it reduced reflections and improved accuracy. Other further improvements include polarized filters, which were not tested. Polarized filters increase clarity. The RTK positioning system depicted in Fig. 15 utilized very critical geolocation with inspection at very short distances.

The reference antenna for RTK functionality was placed on a tripod at a known geodetic reference point. The important results obtained from the field campaigns were that:

- Takeoff for the UAS shall be performed in proximity to the RTK reference antenna, since this allows optimal link stability.
- Takeoff points near the runway threshold allow operations with higher efficiency.

Comparison of results with the conventional inspections by the flight inspection team demonstrated the feasibility of the UAS approach.

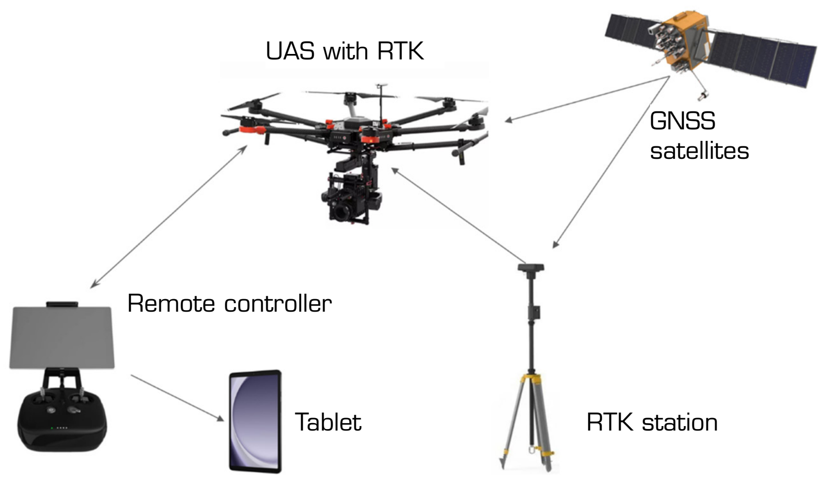

Source: Elaborated by the authors.

Figure 15. Real-time kinematic (RTK) positioning system used for precise geolocation.

Unmanned aerial systems - based PAPI inspection campaigns

The proposed UAS-based PAPI inspection follows a structured methodology, using specialized software that allows well-defined operational procedures. This software was registered with the National Institute of Industrial Property (Instituto Nacional de Propriedade Industrial [INPI]) on September 15, 2023, under the number BR 51 2023 002743 8 0, titled PAPI Inspection Using Remotely Piloted Aircraft. The 3D positional data from the UAS was collected from the RTK using a tablet-based application that can also register the light transition events of the PAPI system. After processing the obtained data, the application calculates the transition angles and produces simplified reports. The inspection procedures consisted of a structured approach containing vertical maneuvers aiming to assess the glide slope angle, as well as horizontal maneuvers to assess horizontal beam coverage, as identified in the previous section.

Inspections using UAS were carried out for validation of the methodology in various types of operational conditions at several aerodromes. The aerodromes where the procedures were performed and the basic information about them are included in Table 2.

Table 2. Information on the aerodromes where UAS-based measurement campaigns were carried out.

Airport location	Campaign period (DD.MM.YYYY)	Runways assessed	ICAO location indicator
Uberlândia	09.11.2020 to 13.11.2020	2 (04, 22)	SBUL
Uberaba	09.11.2020 to 13.11.2020	2 (17, 35)	SBUR
Navegantes	25.11.2020 to 29.11.2020	2 (07, 25)	SBNF
Pelotas	25.11.2020 to 29.11.2020	1 (06)	SBPK
Ilhéus	08.03.2021 to 12.03.2021	2 (11, 29)	SBIL

Source: Elaborated by the authors.

The vertical scanning procedure consisted of the UAS making vertical ascents and descents to capture accurately the transitions of the PAPI lights. One recommended approach is to make at least seven runs to ensure the reliability of the data. Figure 16 shows the process for vertical scanning, including input parameters such as UAS altitude, recorded transition events, and calculated glide slope angles. This increases the visibility of the transition changes and enhances contrast. A blue optical filter enhances this effect for improved detection accuracy. Real-time kinematic (RTK)-global navigation satellite systems (GNSS) positioning ensured precise georeferencing of the detected events and provided the required accuracy to achieve inspection requirements.

During the horizontal scanning process, the UAS flew at a constant height in a sideway motion in such a way that it covered the complete horizontal beam spread of the PAPI lights. The UAS was initially positioned to view all red lights and moved laterally in progressive steps until the lights were not visible. The instant that all lights were on and the instant the first light went out were noted. Figure 17 shows a diagram of the processing chain for horizontal scanning.

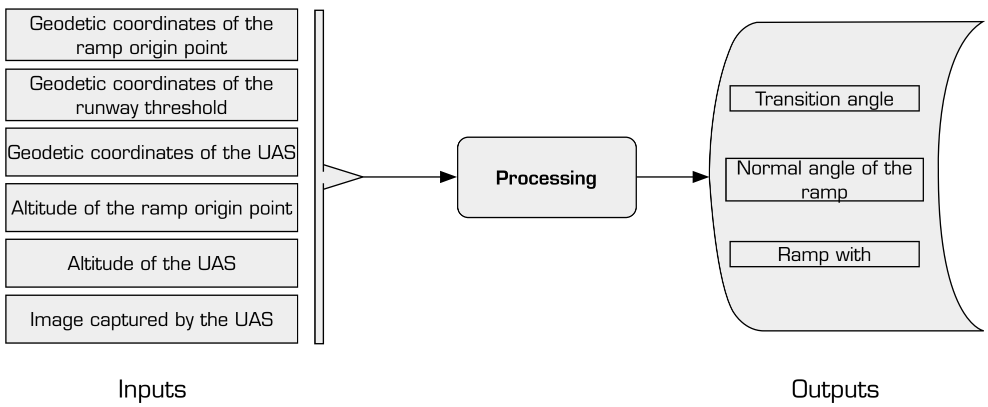

Source: Elaborated by the authors.

Figure 16. Vertical scanning processing diagram.

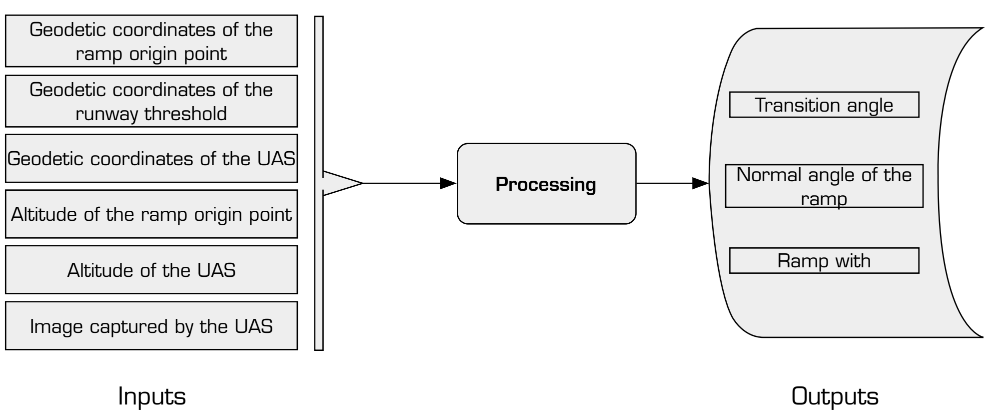

Source: Elaborated by the authors.

Figure 17. Horizontal scanning processing diagram.

Unmanned aerial systems - based PAPI inspections

This section presents the results of six flight inspection experiments at runway thresholds carried out at the following airports: Uberlândia, Uberaba, Navegantes, Pelotas, and Ilhéus. Results will show a comparison of the transition angles, glide slope angles, and angular coverage collected using the traditional flight inspection method performed by the flight inspection squad on crewed flight inspection aircraft with data gathered from the UAS-based methodology using the DJI Matrice 600. This will be done for the purpose of establishing how feasible and reliable the UAS can be as a complementary or alternative solution to the inspections of the PAPI. The definitions of the measurements are provided in the "Conventional PAPI inspection" and "Simulation and constraints" sections for the box angles and "Angular coverage analysis: horizontal scanning" for the horizontal angular coverage.

Vertical and horizontal maneuvers were performed in the campaigns in order to evaluate the glide slope angle and angular coverage, respectively, as described in the "Methodology for UAS-based PAPI flight inspection" section. The data was collected by means of a tablet-based application that measured the 3D positional data provided by the RTK aboard the UAS and detected light transition events from the PAPI system. From the processed data, simplified reports were generated containing key parameters regarding transition angles and angular coverage.

Environmental conditions posed significant challenges during field campaigns, often impacting the inspection process. Adverse weather conditions, such as rain and fog, reduce the few flight opportunities, affecting data acquisition. On the other hand, daylight conditions may lead to poor visibility of light transitions due to conditions that involve the sun aligned with the PAPI system. Such conditions might cause erroneous measurements and were responsible for preventing the procedure to measure the angular coverage on both runways of Uberlândia (SBUL) and Ilhéus (SBIL).

These observations point out that flight inspection operations must be carefully planned to minimize environmental constraints and ensure reliable data collection. Future implementations of UAS-based inspections should take into consideration optimal timing and environmental assessments to enhance the accuracy and consistency of the inspections.

Tables 3 to 7 summarize the results of the campaigns with transition angles and angular coverage obtained by both methods. Unmanned aerial systems (UAS)-derived data demonstrated consistent alignment with GEIV. Minor deviations within the acceptable tolerance limit were present to prove the effectiveness of the UAS approach but at the same time showing possible improvements in areas like data processing and consideration of environmental conditions.

Table 3. Uberlândia results (SBUL).

	RWY 04		RWY 22	
PAPI	GEIV	UAS	GEIV	UAS
Box 1	2.48°	2.35°	2.47°	2.39°
Box 2	2.74°	2.76°	2.76°	2.68°
Box 3	3.32°	3.32°	3.30°	3.21°
Box 4	3.65°	3.64°	3.61°	3.55°
Glide path angle	3.03°	3.04°	3.03°	2.95°
Beam width	0.58°	0.56°	0.54°	0.53°

Source: Elaborated by the authors.

Table 4. Uberaba results (SBUR).

	RWY 17		RWY 35	
PAPI	GEIV	UAS	GEIV	UAS
Box 1	2.50°	2.55°	2.54°	2.50°
Box 2	2.85°	2.92°	2.80°	2.78°
Box 3	3.20°	3.20°	3.17°	3.17°
Box 4	3.56°	3.58°	3.50°	3.51°
Glide path angle	3.03°	3.06°	2.99°	2.98°
Beam width	0.35°	0.28°	0.37°	0.39°
Angular coverage (right)	13.47°	11.00°	11.00°	12.00°
Angular coverage (left)	10.45°	12.00°	12.00°	13.00°

Source: Elaborated by the authors.

Table 5. Navegantes results (SBNF).

	RWY 07		RWY 25	
PAPI	GEIV	UAS	GEIV	UAS
Box 1	2.47°	2.28°	2.59°	2.67°
Box 2	2.87°	2.90°	2.89°	2.96°
Box 3	3.16°	3.17°	3.21°	3.24°
Box 4	3.45°	3.44°	3.52°	4.05°
Glide path angle	3.02°	3.04°	3.05°	3.10°
Beam width	0.29°	0.27°	0.32°	0.28°
Angular coverage (right)	11.00°	11.00°	11.12°	10.00°
Angular coverage (left)	15.00°	9.00°	15.00°	9.00°

Source: Elaborated by the authors.

Table 6. Pelotas results (SBIL).

	RWY 06		RWY 24
PAPI	GEIV	UAS	No PAPI on This RWY
Box 1	2.53°	2.44°	
Box 2	2.84°	2.77°	
Box 3	3.19°	3.16°	
Box 4	3.56°	3.48°	
Glide path angle	3.02°	2.97°	
Beam width	0.35°	0.39°	
Angular coverage (right)	11.00°	9.78°	
Angular coverage (left)	10.00°	9.62°	

Source: Elaborated by the authors.

Table 7. Ilhéus results (SBIL)

	RWY 11		RWY 29	
PAPI	GEIV	UAS	GEIV	UAS
Box 1	2.44°	2.22°	2.60°	2.54°
Box 2	2.78°	2.67°	2.86°	2.79°
Box 3	3.16°	3.08°	3.20°	3.11°
Box 4	3.56°	3.57°	3.59°	3.59°
Glide path angle	2.97°	2.88°	3.03°	2.95°
Beam width	0.37°	0.40°	0.34°	0.32°

Source: Elaborated by the authors.

RESULTS AND DISCUSSION

The initial investigation involved an exploratory analysis comparing the results of the measurements with the UAS against those obtained by conventional flight inspection. The analysis focused exclusively on results where the differences fell within the equipment's tolerance margin of 0.1°. The results were grouped according to the following aspects: a) absolute differences between the results obtained from UAS and those obtained from conventional inspection; b) verification of the standard glide slope angle; and c) correlation between the two datasets using Pearson's correlation coefficient. Potential challenges that could arise, and factors contributing to the measured value throughout the campaigns were identified. The factors are installation errors of the PAPI light boxes, interference of surrounding airport infrastructure affecting the RTK system, operator perception of the light transitions, and potential discrepancies in topographic data inputs. Such factors underscore the need for precision in system calibration, data input, and operator training to ensure that flight inspections based on UAS are reliable.

A comparison between the results obtained from the two methodologies, UAS and conventional flight inspection, was made to evaluate the differences in transition angles, glide slope, and angular coverage. The results are summarized in Tables 8 and 9.

Table 8. Comparison between UAS and conventional inspection results.

Aspect	Category	Total	Within tolerance	Proportion
UAS vs. conventional	Overall	54	49	90.74%
Standard glide slope	Glide path angle	9	9	100.00%

Source: Elaborated by the authors.

Table 9. Correlation between UAS and conventional inspection results.

Parameter	Correlation coefficient
Box 1	0.9755
Box 2	0.9198
Box 3	0.9846
Box 4	0.9415
Glide path angle	0.7740
Beam width	0.9388
Overall	0.9952

Source: Elaborated by the authors.

Table 8 indicates that, concerning the absolute differences in measurements between UAS and conventional inspections, only five out of 54 measurements (9.26%) exceeded the 0.1° tolerance margin. As for the standard glide path angle, all measurements remained within the acceptable tolerance limit, demonstrating the high reliability of the UAS-based inspection method.

Table 9 presents the Pearson correlation coefficient, indicating a very strong correlation between the results for both methodologies, with an overall correlation of 0.9952. This high level of agreement between UAS and conventional inspection methods underscores the feasibility of using UAS-based PAPI inspections as a complementary solution for periodic flight inspections.

Following the preliminary exploratory comparison of the two datasets, the random variables were prepared for a more formal statistical analysis was conducted to validate the UAS-based methodology. Given that the traditional methodology employed by the GEIV with crewed aircraft is well-established, controlled, and serves as the official standard for certifying and periodically inspecting navigation aids, it provides an appropriate benchmark for this validation. The results of the analysis considered solely transition angle measurements. Beam width and angular coverage values were omitted from both samples due to limited numbers.

Since the measurements of each PAPI light box were independent and had different nominal reference values, the random variables were defined as the recorded measurement minus the reference value. These variables are presented in Table 10, in the columns GEIV – REF and UAS – REF, representing the deviations from the reference values. In this analysis, the variables are referred to throughout as GEIV and UAS for simplicity. The statistical analysis was performed using boxplots and histograms (Fig. 18), which provide a graphical representation of data distribution, dispersion, and potential outliers. The analysis revealed greater variability in UAS data compared to conventional methods. However, the boxplot shows that the UAS data distribution has a lower bias, with error values closer to zero.

Statistical analysis

To evaluate the statistical similarity between the measurements obtained from the UAS and the flight inspection team, the Kolmogorov-Smirnov (K-S) test was applied. This non-parametric test measures the maximum deviation between the empirical

Table 10. Transition angle measurements and deviations from reference values.

PAPI Box	GEIV	UAS	REF	GEIV-REF	UAS-REF
1	2.48°	2.35°	2.42°	0.06°	-0.07°
	2.47°	2.39°	2.42°	0.05°	-0.03°
	2.50°	2.55°	2.50°	0.00°	0.05°
	2.54°	2.50°	2.50°	0.04°	0.00°
	2.47°	2.28°	2.50°	-0.03°	-0.22°
	2.59°	2.67°	2.50°	0.09°	0.17°
	2.53°	2.44°	2.50°	0.03°	-0.06°
	2.44°	2.22°	2.50°	-0.06°	-0.28°
	2.60°	2.54°	2.50°	0.10°	0.04°
2	2.74°	2.76°	2.75°	-0.01°	0.01°
	2.76°	2.68°	2.75°	0.01°	-0.07°
	2.85°	2.92°	2.83°	0.02°	0.09°
	2.80°	2.78°	2.83°	-0.03°	-0.05°
	2.87°	2.90°	2.83°	0.04°	0.07°
	2.89°	2.96°	2.83°	0.06°	0.13°
	2.84°	2.77°	2.83°	0.01°	-0.06°
	2.78°	2.67°	2.83°	-0.05°	-0.16°
	2.86°	2.79°	2.83°	0.03°	-0.04°
3	3.32°	3.32°	3.25°	0.07°	0.07°
	3.30°	3.21°	3.25°	0.05°	-0.04°
	3.20°	3.20°	3.17°	0.03°	0.03°
	3.17°	3.17°	3.17°	0.00°	0.00°
	3.16°	3.17°	3.17°	-0.01°	0.00°
	3.21°	3.24°	3.17°	0.04°	0.07°
	3.19°	3.16°	3.17°	0.02°	-0.01°
	3.16°	3.08°	3.17°	-0.01°	-0.09°
	3.20°	3.11°	3.17°	0.03°	-0.06°
4	3.65°	3.64°	3.58°	0.07°	0.06°
	3.61°	3.55°	3.58°	0.03°	-0.03°
	3.56°	3.58°	3.50°	0.06°	0.08°
	3.50°	3.51°	3.50°	0.00°	0.01°
	3.45°	3.44°	3.50°	-0.05°	-0.06°
	3.52°	4.05°	3.50°	0.02°	0.55°
	3.56°	3.48°	3.50°	0.06°	-0.02°
	3.56°	3.57°	3.50°	0.06°	0.07°
	3.59°	3.59°	3.50°	0.09°	0.09°
			Mean	0.0256°	0.0067°
			SD	0.0403°	0.1299°

Source: Elaborated by the authors.

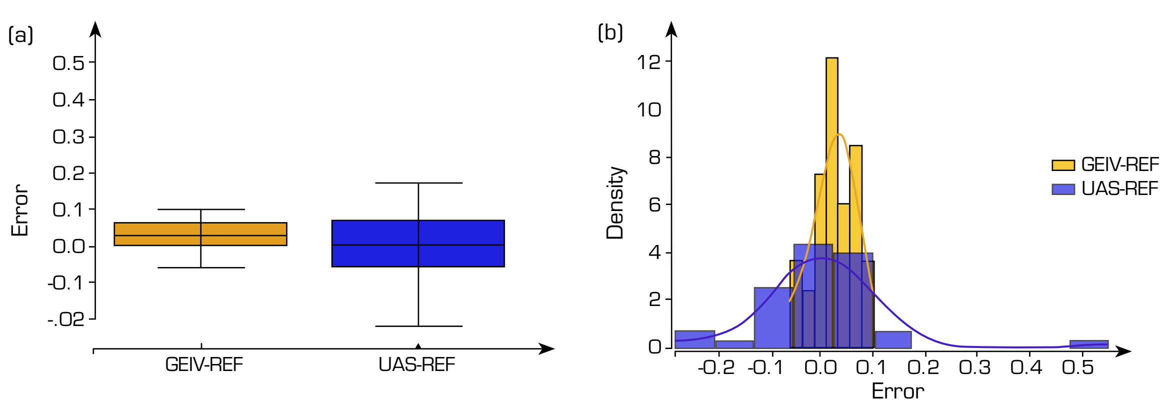

Source: Elaborated by the authors.

Figure 18. Boxplot (a) and histogram (b) of measurement deviations.

cumulative distribution functions (ECDFs) of two datasets, providing a quantitative assessment of whether they originate from the same distribution (Triola 2017).

The analysis process involved ordering the measurement differences, denoted as $X_U = UAS - REF$ and $X_G = GEIV - REF$, in ascending order to construct their respective ECDFs, $F_{nU}(x)$ and $F_{nG}(x)$. The K-S statistic, D_{UG}, represents the largest absolute difference between these functions, given by Casella and Berger (2002):

$$D_{UG} = sup|F_{nU}(x) - F_{nG}(x)| \tag{1}$$

To determine the statistical significance of the observed differences, the critical value, D_{crit}, was calculated using the equation (Casella and Berger 2002):

$$D_{crit} = c(\alpha)\sqrt{\frac{n_G + n_U}{n_G . n_U}} \tag{2}$$

where $c(\alpha)$ is a constant dependent on the chosen significance level α, and n_U and n_G represent the sample sizes for the UAS and GEIV datasets, respectively.

In this work, $\alpha = 0.01$, hence $c(\alpha) = 1.63$. It was found that $D_{UG} = 0.3056$ and $D_{crit} = 0.3842$, with corresponding p-value = 0.0690. Since D_{UG} did not exceed D_{crit} and the p-value was higher than the critical significance level, the null hypothesis of identically distributed both datasets could not be rejected.

These results confirm that the distribution of the measurements obtained by the UAS is statistically consistent with those from the traditional flight inspection method. This overall conclusion provides initial evidence supporting the feasibility of the proposed UAS-based approach for PAPI inspections.

To verify whether the measurement distributions follow a normal distribution, the K-S test was again applied to the distributions of the measurements. In this regard, the ECDF of each dataset X_U corresponding to the UAS measurements and X_G corresponding to the GEIV measurements was tested against a theoretical normal distribution with the same mean and standard deviation (SD). Test statistic D is computed by Eq. 1, but in this case, $D_{UG} = sup|F_n(x) - \Phi(x)|$, where $F_n(x)$ represents the ECDF of the sample and $\Phi(x)$ is the cumulative distribution function of the normal distribution.

At an $\alpha = 0.01$ significance level, $D_{crit} = 0.3842$. The test results of the flight inspection team data yielded a $D_G = 0.1$ and $D_U = 0.1743$ for UAS data, with p-values of 0.8288 and 0.1993, respectively. Since both test statistics were lower than the critical value, and the p-values were greater than the chosen level of significance, the null hypothesis of normality could not be rejected. These results confirm that the distribution of both methods is normal, thereby validating the assumptions necessary for further parametric statistical analysis.

Having confirmed normality in both datasets, the F-test is conducted to determine equality of variances between the two samples. The test compares the variances among the UAS and GEIV measurements to determine whether the differences in those are statistically significant. To calculate the F-statistic (Triola 2017):

$$F = S_U^2 / S_G^2 \tag{3}$$

where S_U^2 and S_G^2 are the sample variances for the UAS and GEIV measurements, respectively. At $\alpha = 0.01$, the critical value of the F-distribution with degrees of freedom $n_U - 1$ and $n_G - 1$ was 2.2309. The results of the test were $F = 10.3781$ with a p-value of 1.8197×10^{-10}, much lower than the significance threshold.

As the obtained F-statistic was greater than the tabulated critical value, the null hypothesis of equality of variances is rejected. Conclusively, this means that the variance of UAS measurements is significantly higher compared to that of GEIV measurements.

This suggests a greater dispersion of results when using UAS for PAPI inspections, which can be visually confirmed by the plot previously depicted in Fig. 18.

Finally, since the two datasets were proven to have unequal variances in the previous analysis, the Welch's t-test was considered for comparison of the mean between the two datasets. It considers unequal variances and calculates a significance of mean measurements difference between the two methods. The test statistic is as presented below (Casella and Berger 2002):

$$T' = \frac{\bar{X}_G - \bar{X}_U}{\sqrt{\left(\frac{s^2{}_G}{n_G} + \frac{s^2{}_U}{n_U}\right)}} \tag{4}$$

where $\bar{X}_G$ and $\bar{X}_U$ are sample means of GEIV and UAS measurements respectively. To account for unequal variances, degrees of freedom were estimated by the Satterthwaite approximation (Casella and Berger 2002):

$$\upsilon' = \frac{\left(\frac{s^2{}_G}{n_G} + \frac{s^2{}_U}{n_U}\right)^2}{\frac{s_G^4}{n^2{}_G(n_G - 1)} + \frac{s_U^4}{n^2{}_U(n_U - 1)}} \tag{5}$$

The critical t-value at α = 0.01 was 2.6990. The test statistic, T' = 0.8334 computed had a p-value = 0.4094. Since the test statistic did not exceed the critical value, and the p-value was above the significance threshold, it was not possible to reject the null hypothesis of the equality of means for both methods. That would mean that, even though the variances are different, the average measurement values from UAS are very close to the ones obtained with conventional inspection methods.

The results of all statistical tests are summarized in Table 11, showing that while the means of the datasets are similar, the UAS data exhibit higher variance.

Table 11. Summary of statistical test results (1% significance level).

Test	Result	p-value
K-S test (distribution)	Same distribution	0.0690
K-S test (normality)	GEIV: normal	0.8288
	UAS: normal	0.1993
Welch's t-test (mean)	Equal means	0.4094
F-test (variance)	Different variances	1.8197×10^{-10}

Source: Elaborated by the authors.

CONCLUSION AND FUTURE WORK

The feasibility study on UAS for PAPI inspections presented promising results, confirming that UAS-based inspections could be an effective, cost-efficient, and sustainable alternative to traditional methods. Results from the comparative analysis of the UAS flight inspection with a traditional flight inspection demonstrated a high level of agreement: 90.74% of the results fell within the equipment's tolerance of 0.1°. The latter suggests that UAS technology can provide precise and reliable measures, especially for a standard glide slope angle, showing full adherence to the defined tolerances.

Detailed statistical analysis has shown that while the UAS-based approach introduces more variability, the mean values remain relatively consistent with those from traditional inspections. Pearson's correlation coefficient of 0.9952 gives further testimony to the strength of the UAS approach and ensures its position as a potential complementary solution for periodic PAPI inspections.

While these findings are positive, system calibration, operational procedures, and environmental factors were also identified as presenting challenges. Variability in UAS measurements indicates that further research development in data processing algorithms, sensor integration, and operator training is required to improve overall accuracy and consistency. Furthermore, the success of UAS-based inspections relies on regulatory acceptance and the establishment of operational guidelines to ensure compliance with aviation standards.

The UAS-based methodology operational advantages include reduced operating cost, less impact on the environment due to reduced fuel consumption, and flexibility in scheduling inspections. All these benefits are aligned with global sustainability and toward attaining the United Nations Sustainable Development Goals, specifically SDG 9 on Industry, Innovation, and Infrastructure, and SDG 13 on Climate Action.

Other potential areas of work for the future are in the integration of multisensory systems, like thermal imaging and LiDAR, that would significantly increase the precision of UAS-based inspections. Moreover, AI-driven data analysis with real-time transmission capabilities may also be considered to ensure better decision-making and operational efficiency. Other navigation aids, like ILS and VOR, may also offer new opportunities to modernize flight inspection processes using UAS.

The inspection methodology using UAS for PAPI has been quite effective to date, serving as an alternative to traditional inspections, especially for remote areas, smaller aerodromes, or as a supplemental tool for conventional flight inspection teams. However, all these benefits are to be availed when further research and technological advancements are performed on the existing challenges to ensure full-scale use of UAS in flight inspection operations. Further refinements are yet needed, with due consideration at the level of regulations, before wide-scale adoption and operational scaling can be considered.

CONFLICT OF INTEREST

Nothing to declare.

AUTHORS' CONTRIBUTION

Conceptualization: Tostes ASM, Marini-Pereira L, Moraes AO, Peixoto LO, Dietzsch G, Smidt CS, Lacerda MG, Habermann M; **Data Curation:** Tostes ASM, Peixoto LO, Smidt CS; **Formal Analysis:** Marini-Pereira L, Tostes ASM; **Funding Acquisition:** Moraes AO, Peixoto LO, Smidt CS; **Investigation:** Tostes ASM, Peixoto LO, Dietzsch G, Smidt CS, Lacerda MG, Habermann M; **Methodology:** Dietzsch G, Lacerda MG, Habermann M, Smidt CS, Peixoto LO; **Project Administration:** Moraes AO, Marini-Pereira L, Tostes ASM; **Supervision:** Moraes AO, Marini-Pereira L; **Writing – Original Draft:** Tostes ASM, Marini-Pereira L, Moraes AO.

DATA AVAILABILITY STATEMENT

The data will be available upon request.

FUNDING

Conselho Nacional de Desenvolvimento Científico e Tecnológico
Grants Nos: 465648/2014-2, 309389/2021-6

Fundação de Amparo à Pesquisa do Estado de São Paulo
Grant No: 2017/01150–0

ACKNOWLEDGMENTS

We gratefully acknowledge DECEA for facilitating this research, IEAv for its invaluable collaboration, GEIV and the aerodrome operational teams for their essential support and laboratory aircraft, PAME-RJ for lending the portable PAPI system, and ICEA with the provision of UAS equipment and specialists, with special thanks to Marcelo Glaucio and Milton Abrunhosa for their decisive contributions in software development and technical and operational expertise.

REFERENCES

Borges SFDS, Cardoso Junior MM, Castilho DS (2024) Method for defining the automation level of an eVTOL. J Aerosp Technol Manag 16:e2224. https://doi.org/10.1590/jatm.v16.1342

Brasil. Ministério da Ciência e Tecnologia (2010) Emissões de gases de efeito estufa no transporte aéreo: segundo inventário brasileiro de emissões e remoções antrópicas de gases de efeito estufa (relatórios de referência). Brasília, DF: Ministério da Ciência e Tecnologia.

Brasil. Ministério da Defesa. Comando da Aeronáutica. Departamento de Controle do Espaço Aéreo (2023) Manual de inspeção em voo. Rio de Janeiro: DECEA.

Casella G, Berger RL (2002) Statistical inference. 2nd ed. Pacific Grove: Duxbury.

Černý M, Tlučhoř T, Hamza M (2022) Methodology for inspecting the correctness of the function of airport lighting systems using a commercially available UAS. Paper presented 2022 New Trends in Aviation Development. IEEE; Piscataway, Slovakia. https://doi.org/10.1109/NTAD57912.2022.10013542

Guardian Jet (2022) Embraer Legacy 500 specifications and summary (S/N 55000043, N543EE). Guardian Jet. [accessed Feb 12 2025]. www.guardianjet.com

DJI (2020) Matrice 300 RTK - user manual. Versão 1.0. [accessed Feb 12 2025]. https://dl.djicdn.com/downloads/matrice-300/20200507/M300_RTK_User_Manual_EN.pdf

Lin YC, Hasheminasa SM, Bullock JL, Horton D, Baxmeyer A, Habib A, Bullock DM (2020) UAS based methodology for measuring glide slope angles of airport precision approach path indicators (PAPI). Paper presented 2020 International Conference on Unmanned Aircraft Systems. IEEE; Piscataway, Slovakia. https://doi.org/10.1109/ICUAS48674.2020.9214049

Marini-Pereira L, Pullen S, Moraes ADO, Sousasantos J (2021) Ground-based augmentation systems operation in low latitudes-part 1: challenges, mitigations, and future prospects. J Aerosp Technol Manag 13:e4621. https://doi.org/10.1590/jatm.v13.1236

Monico JFG, Paula ERD, Moraes ADO, Costa E, Shimabukuro MH, Alves DBM, Souza JR, Camargo PO, Prol FS, Vani BC, et al. (2022) The GNSS NavAer INCT project overview and main results. J Aerosp Technol Manag 14:e0722. https://doi.org/10.1590/jatm.v14.1249

Nowak D, Kopecki G, Kordos D, Rogalski T (2022) The PAPI lights-based vision system for aircraft automatic control during approach and landing. Aerospace 9(285). https://doi.org/10.3390/aerospace9060285

Oliveira Costa D, Oliveira NMF, D'Amore R (2020) The feasibility of remotely piloted aircrafts for VOR flight inspection. Sensors 20(7):1947. https://doi.org/10.3390/s20071947

Oliveira D, Moraes A, Cardoso Junior M, Marini-Pereira L (2023) Safety analysis of RNP approach procedure using fusion of FRAM model and Bayesian belief network. J Navig 76(2-3): 286-315. https://doi.org/10.1017/S0373463323000152

Rahnama E, Asaadi M (2023) Pre-flight check NAV aids system using UAV. Iran airports and air navigation company. ICASC. [accessed Feb 12 2025]. https://www.icasc.co/wp-content/uploads/2023/02/Pre-Flight-Check-NAV-Aids-System-Using-UAV.pdf

Rahnama E, Asaadi M, Parto K (2018) Pre-flight checks of navigation systems and PAPI lights using a UAV. Paper presented 2018 Integrated Communications, Navigation, Surveillance Conference. IEEE; Piscataway, Slovakia. https://doi.org/10.1109/ICNSURV.2018.8384839

Rodrigues RG, Fulindi JB, Oliveira DBPD, Moraes ADO, Marini-Pereira L (2022) Safety analysis of GNSS parallel runway approach operation at Guarulhos International Airport. J Aerosp Technol Manag 14:e1622. https://doi.org/10.1590/jatm.v14.1260

Sivakumar M, Tyj NM (2021) A literature survey of unmanned aerial vehicle usage for civil applications. J Aerosp Technol Manag 13:e4021. https://doi.org/10.1590/jatm.v13.1233

Sommer D, Irigireddy ASCR, Parkhurst J, Pepin K, Nastrucci ER (2020) UAV-based measuring system for terrestrial navigation and landing aid signals. Paper presented 2020 AIAA/IEEE Digital Avionics Systems Conference. IEEE; Piscataway, Slovakia. https://doi.org/10.1109/DASC50938.2020.9256447

Sousasantos J, Marini-Pereira L, Moraes ADO, Pullen S (2021) Ground-based augmentation system operation in low latitudes – Part 2: space weather, ionospheric behavior and challenges. J Aerosp Technol Manag 13:e4821. https://doi.org/10.1590/jatm.v13.1237

Togola S, Kiemde SMA, Kora AD (2021) Real time and post-processing flight inspection by drone: a survey. Adv Sci Technol Eng Syst J 6(3):92-99. https://doi.org/10.1109/TSP49548.2020.9163498

Triola MF (2017) Elementary statistics. 13th ed. Boston: Pearson.

Wikipedia (2023) Precision approach path indicator. Wikipedia. [accessed Feb 12 2025]. https://en.wikipedia.org/wiki/Precision_approach_path_indicator

Wilkens CS, Heinke T, Seide R (2018) Application of unmanned aircraft systems as an instrument in flight inspection. Paper presented 2018 International Flight Inspection Symposium. ICASC; Monterey, USA.

Yadav DK, Kannan P, Mansor S (2022) Evaluating an aircraft response to disturbances caused by vibration frequency of wind forces during landing. J Aerosp Technol Manag 14:e1822. https://doi.org/10.1590/jatm.v14.1261